Pharmaceutical Research (2019) 36: 171
https://doi.org/10.1007/s11095-019-2708-2

RESEARCH PAPER

Physiologically Based Pharmacokinetic Modeling of Oxycodone in Children to Support Pediatric Dosing Optimization

Liang Zheng[1] • Miao Xu[1] • Shi-wei Tang[2] • Hao-xin Song[3] • Xue-hua Jiang[1] • Ling Wang[1]

Received: 4 July 2019 / Accepted: 24 September 2019 / Published online: 25 October 2019

ABSTRACT

Purpose Physiologically-based pharmacokinetic (PBPK) modeling offers a unique modality to predict age-specific pharmacokinetics. The objective of this study was to assess the ability of PBPK model to predict plasma exposure of oxycodone, a widely used opioid for pain management, in adults and children.

Methods A full PBPK model of oxycodone following intravenous and oral administration was developed using a 'bottom-up' and 'top-down' combined strategy. The model was then extrapolated to pediatrics through a reasonable scaling method. The adult and pediatric model was evaluated using data from 17 clinical PK studies by testing predicted/observed goodness of fit. The mean fold error for PK parameters was calculated. Finally, we used the validated PBPK model to visualize adult-children dose conversion for oxycodone.

Results The developed PBPK model successfully predicted the oxycodone disposition in adults, wherein the predicted *versus* observed AUC, $C_{max,}$ and t_{max} were within 0.90 to 1.20-fold difference. After scaling anatomy/physiology, protein binding, and clearance, the model showed satisfactory prediction performance for pediatric populations as predicted AUC were within the 1.50-fold range of the observed values. According to the application of PBPK model, we found that different intravenous doses should be given in children of different ages compared to a standard 0.1 mg/kg in adults, while a progressive increasing dose with age growth following oral administration is recommended for children.

Conclusions The current example provides the opportunity for using the PBPK model to guide dose adjustment of oxycodone in the design of future pediatric clinical studies.

KEY WORDS dosing regimen · oxycodone · PBPK modeling · pediatric

INTRODUCTION

The rational use of pediatric medicine is a challenge mainly because of the lack of enough information on pharmacokinetic (PK) profiles in children. The rapid changes in drug disposition due to physiological and metabolic development over childhood had been reported and characterized as an essential factor for pediatric dose design (1,2). Traditional pediatric dosing methods based on body weight or age alone are not able to fully reflect specific organ and clearance maturation. Using empiric models paired with 3/4 power allometry does a fairly good job though maturation remains unaccounted for younger children whose clearance could be overpredicted (3,4). Physiologically based pharmacokinetic (PBPK) modeling has been proven to be a valuable tool in drug development and regulatory assessment, as it offers the opportunity to simulate the PK of a compound, with a mechanistic understanding, in various populations and medical statues (5). Utilization of PBPK for logical extrapolation across the age continuum has been recommended by drug regulatory authorities. Of the 254 applications reviewed by FDA's Office of Clinical

Electronic supplementary material The online version of this article (https://doi.org/10.1007/s11095-019-2708-2) contains supplementary material, which is available to authorized users.

✉ Ling Wang
rebeccawang312@gmail.com

[1] Department of Clinical Pharmacy and Pharmacy Administration, West China School of Pharmacy, Sichuan University, Chengdu, China

[2] Department of Pharmacy, People's Hospital of Dujiangyan City, Dujiangyan, China

[3] Department of Pharmacy, West China Second Hospital of Sichuan University, Chengdu, China

Pharmacology which incorporated PBPK into their submission, 15% are intended to mimic PK among children (6).

Pain management in the pediatric population is complicated with unique challenges in dosing management, especially for high-risk opioids (7). Because of their potential to cause addiction and serious consequences with overdosing, opioids usage is closely monitored and strictly controlled in clinical practice. In spite of progressing in the understanding of opioid PK in children, limited data about the safety and effectiveness of these agents still exist. Oxycodone is a semisynthetic opioid with similar structure to codeine synthesized in 1916 and has been widely used for pain management (8). In 2008, oxycodone consumption surpassed morphine, and in 2012, oxycodone accounted for nearly 50% of global consumption of total opioids (9). Use of oxycodone has a long history in pediatric patients. Per-oral oxycodone preparations, both immediate-release (IR) and controlled-release (CR) formulations, have recently been approved for pediatric patients over 11 years old, while intravenous bolus remains the standard route for younger children (9).

Previous PK studies demonstrated that oxycodone is extensively metabolized in the liver into noroxycodone and oxymorphone by cytochrome P450 (CYP) 3A4/5 and 2D6, respectively. Apart from oxidative reactions, it also directly undergoes glucuronidation catalyzed by UDP-glucuronosyltransferases (UGT) 2B7 and UGT2B4 (10,11). The metabolites contribute little to the anesthetic effect compared to the parent form. Oxycodone has an oral bioavailability of about 60% and can be eliminated within 24 h following intravenous (i.v.) dosing and oral (p.o.) administration of IR formulations (12,13).

It is important to know PK profiles in specific populations for individualized dose regimens. Though an adult oral PBPK model for oxycodone has been reported before, this study aims to develop an oxycodone PBPK model in children (14). We used an age-related scaling method to implement the adult-children model extrapolation. The pediatric PK profiles collected from the literature provided the necessary *in vivo* data to evaluate prediction performance. Using the validated model, we designed a virtual clinical trial to facilitate pediatric dose optimization by comparing with plasma exposure in adults.

METHODS

PBPK Development Workflow, Clinical Data, and Software

In this study, a guidance-based workflow for PBPK model development in children was adopted (3). A 'bottom-up' and 'top-down' combined strategy was used to facilitate model establishment (Fig. 1). First, a PBPK model for oxycodone in the adult population after intravenous and oral administration was developed and evaluated. Afterwards, the established adult PBPK model was extrapolated to the pediatric population by adjusting anatomical and physiological parameters using age-dependent algorithms. In this stage, the physicochemical and absorption, distribution, metabolism, and excretion (ADME) properties of oxycodone remained the same. The simulated plasma exposure of virtual populations was compared with the observed concentration data to assess the accuracy of the PBPK model. When the final model was verified, we simulated a PK study for pediatric dose optimization. The reported PK profiles following intravenous and oral administration from the literature were obtained by searching Google scholar using terms 'oxycodone', 'pharmacokinetics' and pediatric-specific keywords such as 'children' and 'infant'.

We performed this modeling work with Open Systems Pharmacology Suite version 7.4.0 comprising PK-Sim® and

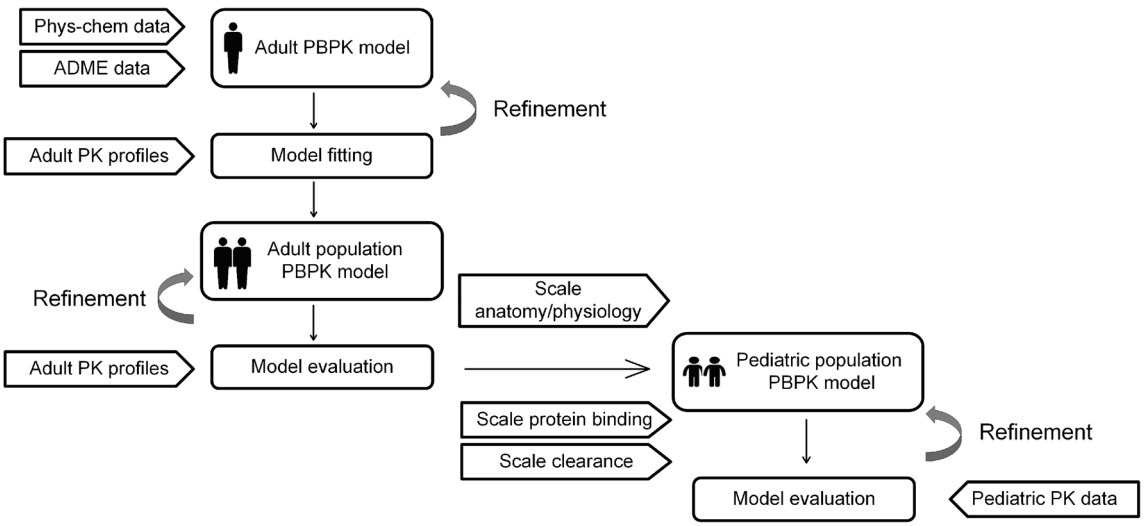

Fig. 1 Diagram for pediatric modeling workflow. Phys-chem, physiochemical; ADME, absorption, distribution, metabolism, and excretion.

Mobi® (Bayer Technology, www.open-systems-pharmacology.org). Parameter identification using the Monte Carlo algorithm was conducted in PK-Sim®. The published plasma concentration-time data were digitized by using GetData Graph Digitizer version 2.25.0.32 (S. Fedorov). PK parameters estimated by the non-compartment analysis were obtained from the literature or using PKanalix® version 2019R1 (Lixoft, Orsay, France). Origin version 2019b (OriginLab, Northampton, USA) and Microsoft Visio were used for graphics creation and compiling.

Adult PBPK Model

Adult Model Development

A generic whole body 18 compartment PBPK model implemented in PK-Sim® was used. Each organ compartment comprises four inner sub-compartments, i.e., blood, plasma, interstitial, and intracellular spaces (15). The physicochemical and ADME parameters of oxycodone are shown in Table 1. The tissue-to-plasma partition coefficients were calculated using the Rodgers and Rowland method (16). The cellular permeabilities (permeabilities between interstitial and cellular space) were predicted by a PK-Sim® standard method. According to the literature, oxycodone is 38–45% protein bound, mainly to albumin (9). Thus, the unbound fraction (f_u) was assumed to be 0.62. The blood to plasma ratio was also obtained from the literature. Three enzymes, namely, CYP3A4, CYP2D6, and UGT2B7, are responsible for metabolism. The clearance process via enzymes can be quantified using the equation (Eq 1):

$$CL_{int,E} = \frac{V_{max}}{K_m + [S]} = \frac{Abundance \times k_{cat}}{K_m + [S]} \quad (1)$$

where $CL_{int,E}$ is intrinsic clearance per unit protein, K_m is the Michaelis-Menten constant, k_{cat} is the turnover number described as maximum reaction rate (V_{max}) per unit enzyme, and [S] is the substrate concentration (17). Abundance is the enzyme concentration in where metabolism takes place. The hepatic reference concentrations of CYP3A4, CYP2D6, and UGT2B7 were set to 4.32, 0.40, and 1.00 µmol/L, respectively (18). The extrahepatic expression of these enzymes was reckoned by multiplying the hepatic reference concentration with relative expression, whose values are provided in the human gene expression database released with the software (19).

We developed the model based upon a typical 25-year-old European male individual with average physiological parameters. Parameter identification was performed to best fit the observed data from the four studies for refinement of initial parameters (13,20–22). These studies include the pharmacokinetic reports in adults after a single i.v. dose of 0.1 mg/kg oxycodone and an *in vivo* mass balance study following a single p.o. administration of 15 mg IR solution (Supplementary Table S1). Specifically, the fraction metabolized was set to

Table I Summary of Input Parameters of Oxycodone PBPK Model

Parameter	Initial value	Source/Method	Final modified value
logP	1.20	Pubchem	2.50
f_u	0.62	(9)	
B/P	1.30	(41)	1.07
MW	315 g/mol	–	
pKa	8.53	Drugbank	
solubility	5.59 mg/ml	Pubchem	
gastric emptying time	40 min	assumed	
specific intestinal permeability	1.16E-5 cm/min	in silico calculation	
$K_{m,CYP3A4}$	670 µM	(10)	
$k_{cat,CYP3A4}$	61.9 l/min	fitted to $f_{m,CYP3A4}$	
$f_{m,CYP3A4}$	0.45	(13)	
$K_{m,CYP2D6}$	39.8 µM	(10)	
$k_{cat,CYP2D6}$	17.0 l/min	fitted to $f_{m,CYP2D6}$	
$f_{m,CYP2D6}$	0.19	(13)	
$CL_{int,UGT2B7}$	0.10 l/min	parameter identification	
GFR fraction	1	fitted to f_{renal}	
tubular secretion	0.08 l/min		
f_{renal}	0.08	(13)	

logP lipophilicity, f_u fraction unbound, *B/P* blood to plasma concentration ratio, *MW* molecular weight, *pKa* acid dissociation constant, K_m Michaelis constant, k_{cat} *in vitro* V_{max} per recombinant enzyme, f_m fraction metabolized by a certain enzyme, CL_{int} intrinsic clearance, *GFR fraction* glomerular filtration fraction, f_{renal} fraction excreted unchanged via kidney

0.45 within 48 h for CYP3A4, and 0.19 for CYP2D6, as the previous study indicated. The intrinsic kidney clearance (CL_R) is the combination of glomerular filtration (GFR) and tubular secretion. Because no evidence shows that oxycodone undergoes re-absorption in the kidney, the renal filtration was set at 1. The total CL_R was corrected according to the observed value of fraction unchanged in the urine, which was 0.08 (13). The remaining was roughly attributed to UGT-mediated metabolism defined as a first-order process given that K_m for UGT metabolism is very high (11).

Oral formulations include IR solution/tablet characterizing the drug as being in solution at the point of administration, and CR tablet whose release feature was described with a Weibull function (Eq. 2) to match the *in vitro* release data (23–25).

$$m = 1 - \exp\left(\frac{-t^{0.5}}{2.3}\right) \tag{2}$$

where m is the accumulated fraction of the drug at the time t (h).

Adult Model Evaluation

For adult model evaluation, 14 clinical reports on oxycodone PK in adults following various dosing regimens were identified and used (Supplementary Table S1). We used the population building block of the software to create all virtual populations that correspond to subject demographics in each clinical study. The simulations were conducted and the predicted concentration-time curves were visually compared with the observed values for an initial check. The performance was evaluated by comparison of predicted to the observed area under the plasma curve (AUC), maximum concentration (C_{max}), and time to reach C_{max} (t_{max}) values. As a quantitative measure, the mean fold error (MFE) was calculated for these PK parameters (Eq. 3).

$$MFE = \frac{\text{Predicted mean}_{\text{parameter}}}{\text{Observed mean}_{\text{parameter}}} \tag{3}$$

The model was accepted if all predicted PK parameters were within 2-fold of the corresponding observed values, as is a commonly used standard (26).

Extrapolation to Pediatric PBPK Model

Anatomical and Physiological Parameters

The pre-built age-dependent algorithms in PK-Sim® based on International Commission on Radiological Protection (ICRP) population data were used to generate respective populations for children with demographic characteristics parallel to those reported in the literature. The adjusted anatomical and physiological parameters body weight, height, organ volume, specific blood flow, hematocrit, total body water, lipid, and protein concentrations were incorporated which represent the mean values of European children.

Scaling Unbound Fraction

The unbound fraction of oxycodone in children was estimated using a default albumin ontogeny function and unbound fraction in adults, as shown in Eq. 4.

$$fu_{child} = \frac{1}{1 + OSF_p \cdot \frac{1 - fu_{adult}}{fu_{adult}}} \tag{4}$$

where fu_{child} and fu_{adult} are unbound fractions of oxycodone for children and adults, respectively, and OSF_p is the age-dependent ontogeny scaling factor of albumin (27).

Scaling Metabolism

A physiologically based mechanistic approach for the scaling of clearance in children was used. The physiologic hepatic clearance scaling is based on the assumption of consistent metabolic pathways between adults and children, well-stirred model conditions, and non-saturable enzyme kinetics.

We used the default ontogeny profiles for CYP2D6, CYP3A4, and UGT2B7 in PK-Sim® (28). In such settings, the activity of hepatic CYP3A4 is estimated to be 12% of the adult at birth and increases to 50% by the age of approximately 0.75 years. It reaches the adult level at 5 years. CYP2D6 has 45% activity at birth and maturates over a postnatal period of 1.8 years. Enzymatic activity of UGT2B7 is less than 2% at term and does not attain 100% activity until 3 years. The following formula (Eq. 5) was used to calculate the scaled pediatric intrinsic clearance for metabolic enzymes:

$$CL_{int,E(child)/gliver} = CL_{int,E(adult)/gliver} \times OSF_{CYP/UGT} \tag{5}$$

where $CL_{int,E(child)/gliver}$ is the respective scaled intrinsic clearance for CYP3A4, CYP2D6, and UGT2B7 per gram of liver; $CL_{int,E(adult)/gliver}$ is the intrinsic clearance for CYP3A4, CYP2D6, and UGT2B7 per gram of liver in adults; $OSF_{CYP/UGT}$ is the ontogeny scaling factor for each enzyme.

Scaling of Renal Clearance

The renal clearance of oxycodone is considered to be a passive process consisting of GFR and tubular secretion without

reabsorption. The pediatric renal clearance of oxycodone is deduced by Eq. 6 and 7:

$$CL_{GFR,child} = \frac{GFR_{child}}{GFR_{adult}} \times \frac{fu_{child}}{fu_{adult}} \times CL_{GFR,adult} \quad (6)$$

$$CL_{TS,child} = \frac{TS_{child}}{TS_{adult}} \times \frac{fu_{child}}{fu_{adult}} \times CL_{TS,adult} \quad (7)$$

where $CL_{GFR,child}$ and $CL_{GFR,adult}$ correspond to renal clearance of oxycodone based on glomerular filtration in children and adults; $CL_{TS,child}$ and $CL_{TS,adult}$ are renal clearance based on tubular secretion, respectively. GFR_{child} and GFR_{adult} are age-specific glomerular filtration of children and adults; TS_{child} and TS_{adult} represent age-specific tubular secretion of children and adults, respectively (28). Because the function for the ontogeny of tubular secretion was based on the excretion of p-aminohippuric acid, we assumed that the ontogeny of tubular secretion of oxycodone would be parallel to that of p-aminohippuric acid (29).

Pediatric Model Performance Evaluation

Kokki *et al.* and Tahtawy *et al.* described the PK of oxycodone after 0.1 mg/kg i.v. and p.o. administration in children aged 6–93 months and 6–88 months, respectively (30,31). Olkkola *et al.* reported the PK in children aged 2–10 years following a 0.1 mg/kg i.v. dose (32). Totally 106 and 82 individual observed values were obtained from Kokki *et al.* and Tahtawy *et al.* respectively, and representative mean values were extracted from Olkkola *et al.* based on visual inspection (Supplementary Fig. S2). For the PBPK model performance verification in children, simulations were conducted and then compared with the observed PK profiles extracted from the three studies. The MFE of PK parameters was calculated as described in section "Adult model evaluation".

Pediatric Dose Optimization

Five virtual pediatric groups with full-term gestation (40 weeks) classified by postnatal age, i.e. newborn (0–1 month), toddler (0.1–2 years), preschool (2–6 years), school age (6–12 years) and adolescent (12–18 years) with 100 individuals each (equal gender), were created using the population building block. We also created an adult population (19–40 years) as a reference. The pediatric dose was optimized to achieve an oxycodone plasma exposure similar (within 15% deviation) to that expected in adults. For i.v. administration, a standard dose of 0.1 mg/kg in adults was adopted as a reference, while a 10 mg IR formulation was used for p.o. dosing.

RESULTS

Adult PBPK Model Evaluation

We built an initial adult PBPK model with the predicted plasma concentrations of oxycodone, and with fractions of metabolized and excreted unchanged in urine, consistent with that of observed data obtained from the European or American adult population aged 19 to 40 (Fig. 2). The model simulated the time-concentration profiles following i.v. dosing of 0.1 mg/kg, and p.o. dosing of 15 mg. The calculated oral bioavailability is 0.61. On visual inspection, the population model well predicted single intravenous administration at a dose of 0.07 mg/kg, oral administration of a 10 mg IR solution/tablet, and oral administration of a 20 mg CR tablet (Fig. 3a-c). The goodness of fit plot demonstrated that 94% of the observed mean concentration values are within the 2-fold error range of the prediction when 70% are within 1.25-fold error range (Fig. 3d). Supplementary Fig. S1 gives the simulation results for single oral dosing of a 15 mg and 20 mg IR solution/tablet, single oral dosing of a 40 mg IR solution/tablet, and multiple oral dosing of a 20 mg CR tablet. All predicted PK parameters are within 1.5-fold of the corresponding observed values (Table 2).

Pediatric PBPK Model Evaluation

By using the scaling method described in the methods, the adult PBPK model was extrapolated to the pediatric population. The age range and sex distribution were similar between the virtual population and children reported in the literature (Table S1). The pediatric model well described the PK feature in children after i.v. and p.o. dosing compared with the observed values (Fig. 4a-e). A proper fitting was obtained, as demonstrated by 96% of the observed mean concentrations falling within the 2-fold error range of the prediction, with 85% within 1.25-fold error range (Fig. 4f). The prediction performance of i.v. model is better than that of p.o. model as determined by MFE, mainly due to several significant outliers in the observed p.o. data (Table 2). All predicted PK parameters are within 1.50-fold of the corresponding observed values.

Virtual Simulation for Pediatric Dose Optimization

We constructed five pediatric groups for dose design. A direct comparison through Box-Whisker analysis was implemented to illustrate the PK variability in children. As shown in Fig. 5a, intravenous doses should be adjusted to 0.07 mg/kg for newborn <1 month of age, 0.12 mg/kg for children >1 month—12 years of age, and 0.1 mg/kg for adolescent aged 12—16 years old, to achieve an approximately equivalent plasma

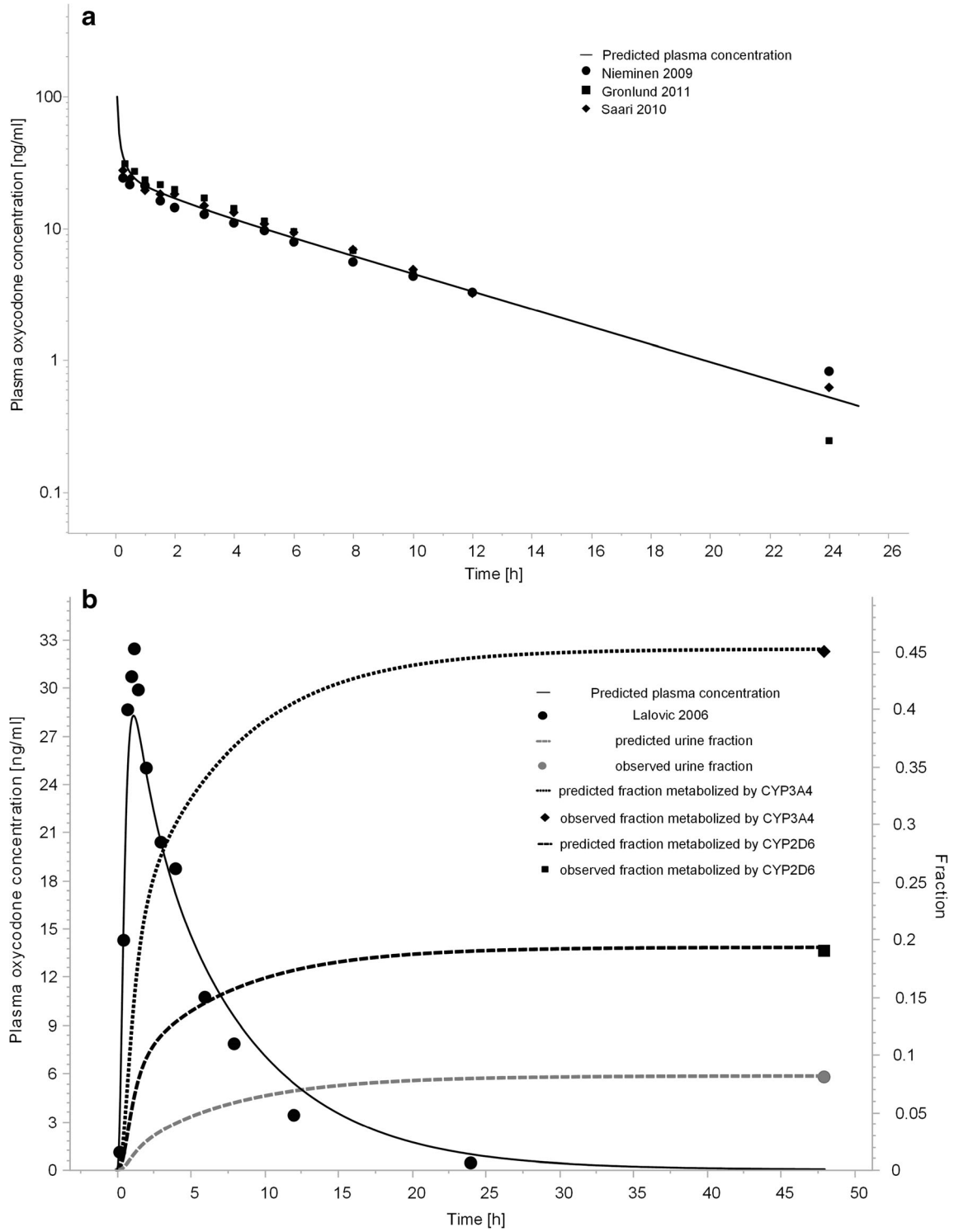

Fig. 2 Simulated and observed plasma time-concentration profiles of oxycodone following 0.1 mg/kg i.v. administration (**a**) and p.o. administration of 10 mg IR tablets (**b**). The simulated curve (solid lines) was predicted from a typical European individual created in the PK-Sim®. The dashed and dotted lines (**b**) represent fraction metabolized by CYP and fraction excreted unchanged into the urine, as indicated by the figure legend.

exposure of oxycodone in adults following 0.1 mg/kg i.v. dosing. The oral doses for children should increase progressively with age growth, i.e., 1.75 mg for toddler, 3 mg for preschool, 5 mg for school age, and 7.5 mg for adolescent, which are comparable to 10 mg IR formulation in adults by using $AUC_{0\text{-}24h}$ as the indicator (Fig. 5b).

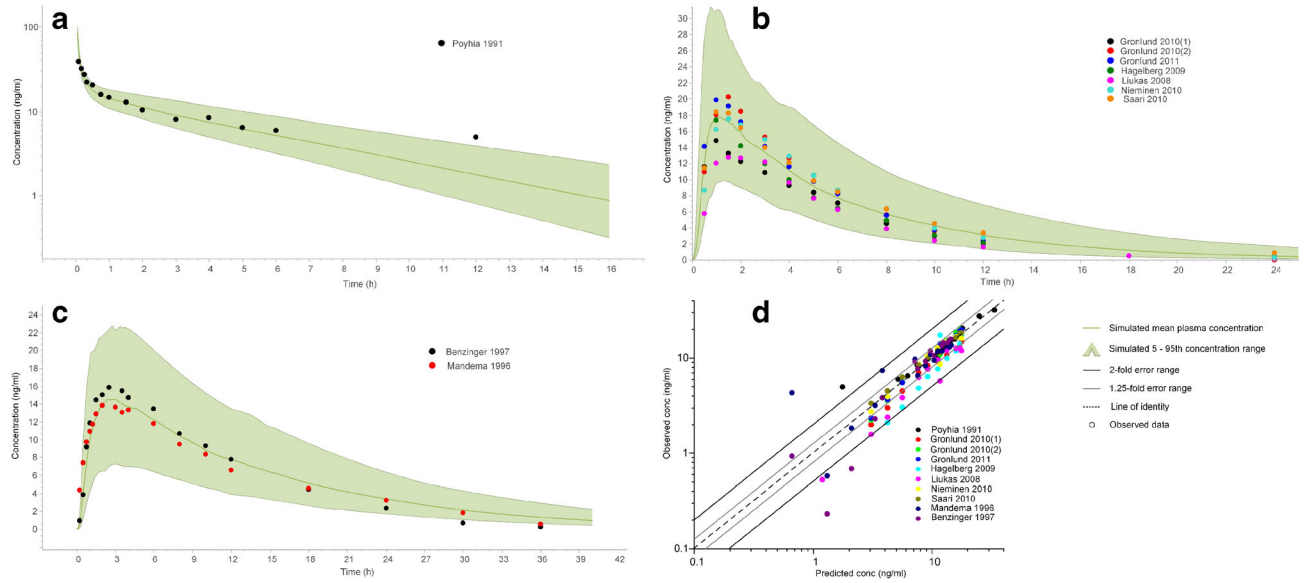

Fig. 3 Population PBPK model verification in healthy adults. (**a**) i.v. administration at a dose of 0.07 mg/kg in European, (**b**) p.o. administration of 10 mg IR solution or tablets in European, (**c**) p.o. administration of 20 mg CR tablets in American. The observed concentration data were provided as the arithmetic mean values extracted from references, as indicated in the figure. Population simulation arithmetic means are shown as lines, and the shaded areas illustrate the 5-95th prediction range. (**d**) The goodness of fit plot for the simulated oxycodone plasma concentrations in populations of healthy adults.

DISCUSSION

The population PBPK model that incorporates pediatric changes in anatomical, physiological, and biological parameters is a valuable alternative for empirical dosage selection when there is no adequate clinical data in children. To our knowledge, we are the first to develop a pediatric PBPK model to predict PK profiles of oxycodone in children of all age stages. Our model was first validated using previous clinical PK studies, increasing the reliability of the simulation of the PK profiles with various dosing regimens.

Our model well predicted the PK of oxycodone in adults following single i.v. administration of 0.07 and 0.1 mg/kg solution, single p.o. administration of 10, 15, 20 and 40 mg IR formulation, and single and multi-dose of 20 mg CR tablet, over a wide concentration range (Fig. 3 and Fig. S1). The model also captured the PK feature of oxycodone in children with different age brackets after i.v. and p.o. dose of 0.1 mg/kg, indicating that the proposed scaling method is suitable for age-dependent PK prediction (Fig. 4). Apart from anatomical and physiological change, the clearance process linked to metabolic enzymes and renal excretion is mechanistically adjusted with the ontogeny of enzymes and organs. This method considered the growing drug clearance in children and has been proved to gain an advantage over traditional pediatric dosing methods only based on body weight or age (3). As indicated in the results, i.v. dose predicted by the PBPK model varies according to the age stage. The newborn should have a lower dose while toddler, preschool, and school-age children are suggested to have a higher dose compared with adults to reach similar drug exposure (Fig. 5a). Our finding is consistent with the previous study, which claimed that the PK in children following i.v. dosing is generally similar to that in adults, but that neonates have a slower clearance while older infants have a slightly faster clearance (9). However, the model predicts that oral bioavailability after a single dose of 10 mg IR formulation in adults and children at different stages varied from 0.58 to 0.65 (data not shown), indicating that age has a minor impact on oxycodone bioavailability. From p.o. dose prediction, we found several severe outliers in the toddler group (Fig. 5b). According to the current knowledge, we think that younger children have greater PK variability theoretically since they experience the most critical period for maturation of the drug disposition system with a nonnegligible personal difference (1,33,34). For instance, the ontogeny profiles of three enzymes mainly responsible for oxycodone metabolism (CYP3A4, CYP2D6, and UGT2B7) reveal a significant change of metabolic activity with considerable individual differences in this stage. As proof, our model predicts a broader variation range of oxycodone exposure in the newborn and toddler. Despite these variations, our study offers a unique tool to produce valuable information for pediatric dose design.

The strategy for the initial model establishment in this study is slightly different from the protocol instruction (35). In general, it should start with i.v. model since this route does not require consideration of gastrointestinal absorption. However, an extensive *in vivo* biotransformation and mass balance study of oxycodone which provided crucial information for model refinement was conducted after oral consumption only. The PBPK model could also be developed solely for oral application depending on the situation (35). Therefore, we

Table 2 Predicted (Pre) and Observed (Obs) Pharmacokinetic Parameters of Oxycodone in Different Populations and Dosing Regimen. Results Expressed as Arithmetic Mean Parameters

Population	Study reference	Dose		$AUC_{0-\infty}$ (μg·min/ml)	C_{max} (ng/ml)	t_{max} (h)
Healthy adult		0.07 mg/kg i.v.	Predicted	5.75	–	–
	Poyhia 1991 (42)		Observed	6.00	–	–
			pre/obs ratio	0.96	–	–
	Adult i.v. MFE			0.96		
		10 mg IR p.o.	Predicted	7.31	17.7	1.10
	Gronlund 2010 (37)		Observed	5.70	18.0	1.00
			pre/obs ratio	1.28	0.98	1.10
	Gronlund 2010 (43)		Observed	7.50	21.5	1.50
			pre/obs ratio	0.97	0.82	0.73
	Gronlund 2011 (44)		Observed	7.30	22.5	1.00
			pre/obs ratio	1.00	0.79	1.10
	Hagelberg 2009 (45)		Observed	6.10	18.1	1.00
			pre/obs ratio	1.20	0.98	1.10
	Liukas 2008 (46)		Observed	5.10	15.2	1.90
			pre/obs ratio	1.43	1.16	0.58
	Nieminen 2010 (47)		Observed	7.30	18.9	1.50
			pre/obs ratio	1.00	0.94	0.73
	Saari 2010 (21)		Observed	7.14	18.8	1.00
			pre/obs ratio	1.02	0.94	1.10
		15 mg IR p.o.	Predicted	11.0	26.6	1.00
	Nieminen 2009 (20)		Observed	10.7	26.1	1.50
			pre/obs ratio	1.03	1.02	0.67
	Nieminen 2010 (48)		Observed	11.6	33.6	1.25
			pre/obs ratio	0.95	0.79	0.8
	Lalovic 2006 (13)		Observed	10.8	38.0	1.08
			pre/obs ratio	1.02	0.70	0.93
		20 mg IR p.o.	Predicted	14.3	31.5	1.30
	Mandema 1996 (49)		Observed	11.7	41.6	1.30
			pre/obs ratio	1.22	0.76	1.00
		40 mg IR p.o.	Predicted	28.7	63.1	1.20
	Webster 2012 (50)		Observed	26.8	82.1	1.60
			pre/obs ratio	1.07	0.77	0.75
	Setnik 2017 (51)		Observed	22.7	65.0	1.00
			pre/obs ratio	1.26	0.97	1.20
		20 mg CR p.o.	Predicted	14.0	14.6	2.90
	Benziger 1997 (52)		Observed	12.5	15.8	2.50
			pre/obs ratio	1.12	0.92	1.16
	Mandema 1996 (49)		Observed	12.0	18.6	2.62
			pre/obs ratio	1.17	0.78	1.11
	20 mg CR p.o. q 12 h*		Predicted	7.15	12.8	2.30
	Reder 1996 (53)		Observed	6.22	15.1	3.20
			pre/obs ratio	1.15	0.85	0.72
	Adult p.o. MFE			1.12	0.89	0.92
Children	Kokki 2004 (30)	0.1 mg/kg i.v.	Predicted	6.40	–	–
			Observed	6.61	–	–
			pre/obs ratio	0.97	–	–
	Tahtawy 2006 (31)		Predicted	6.14	–	–
			Observed	6.25	–	–

Table 2 (continued)

Population	Study reference	Dose		$AUC_{0-\infty}$ (μg·min/ml)	C_{max} (ng/ml)	t_{max} (h)
			pre/obs ratio	0.98	–	–
	Olkkola 1994 (32)		Predicted	6.63	–	–
			Observed	5.67	–	–
			pre/obs ratio	1.17	–	–
	Children i.v. MFE			1.04		
	Kokki 2004 (30)	0.1 mg/kg p.o.	Predicted	4.23	13.7	1.20
			Observed	2.44	9.20	3.22
			pre/obs ratio	1.73	1.49	0.37
	Tahtawy 2006 (31)		Predicted	3.86	–	–
			Observed	3.96	–	–
			pre/obs ratio	0.97	–	–
	Children p.o. MFE			1.35	–	–

AUC area under the concentration-time curve, C_{max} maximum concentration, t_{max} time to reach maximum concentration, *MFE* mean fold error calculated by dividing the predicted means by observed means of PK parameters, *IR* immediate-release solution or tablet, *CR* controlled-release tablet. The mean parameters were obtained directly from references if available or calculated by non-compartment analysis using the observed data. *, calculated from the administration time of the last dose

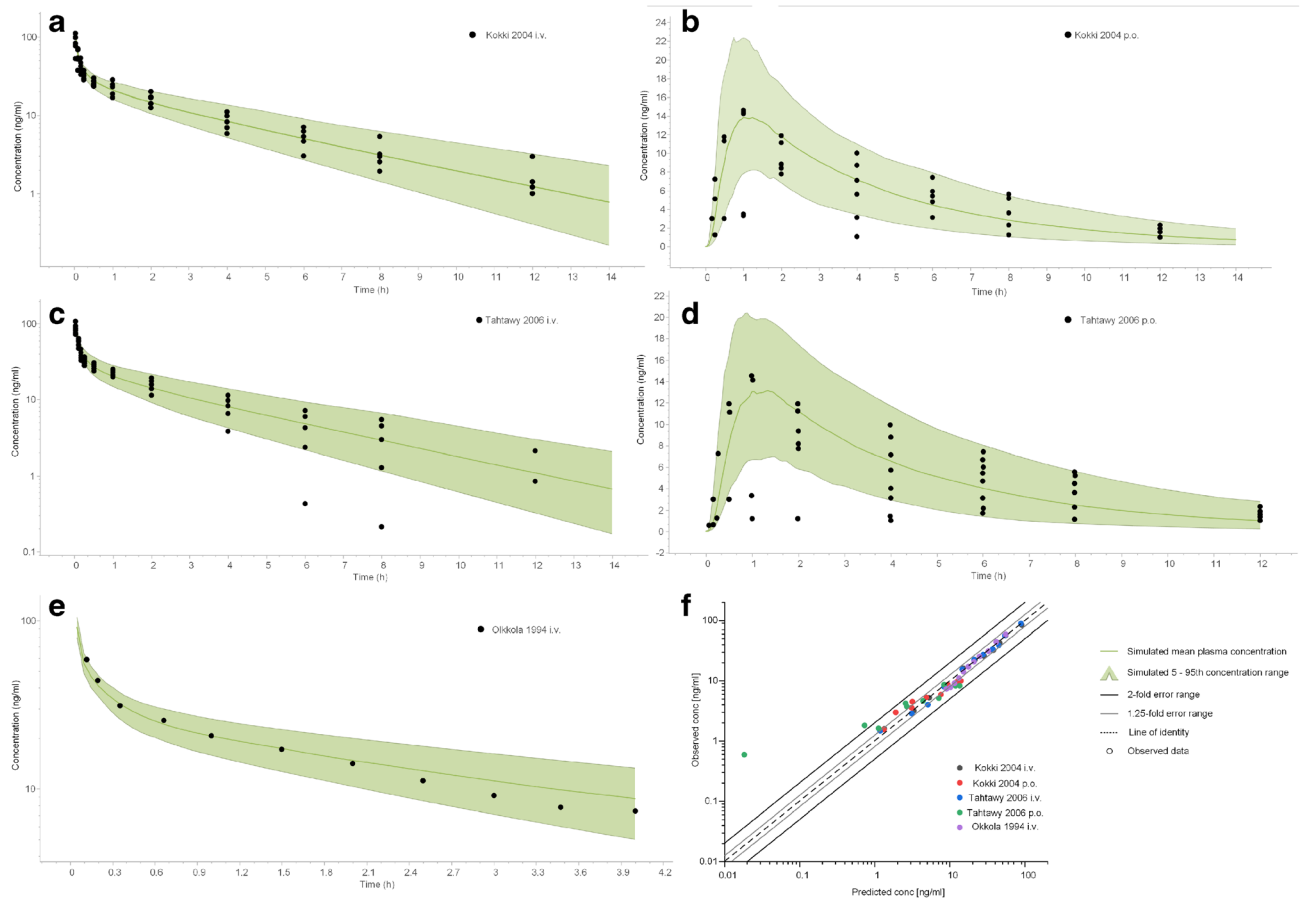

Fig. 4 Population PBPK model verification in children. (**a**) & (**b**) 0.1 mg/kg i.v. and p.o. administration in children aged 6–93 months, respectively; (**c**) & (**d**) 0.1 mg/kg i.v. and p.o. administration in children aged 6–88 months, respectively; (**e**) 0.1 mg/kg intravenous administration in children aged 2–10 years. Observed individual data were obtained from Kokki 2004 and Tahtawy 2006, while mean concentration values estimated from Olkkola 1994 on visual inspection. Population simulation arithmetic means are shown as lines, and the shaded areas illustrate the 5-95th prediction range. (**f**) The goodness of fit plot for the simulated oxycodone plasma concentrations in pediatric populations.

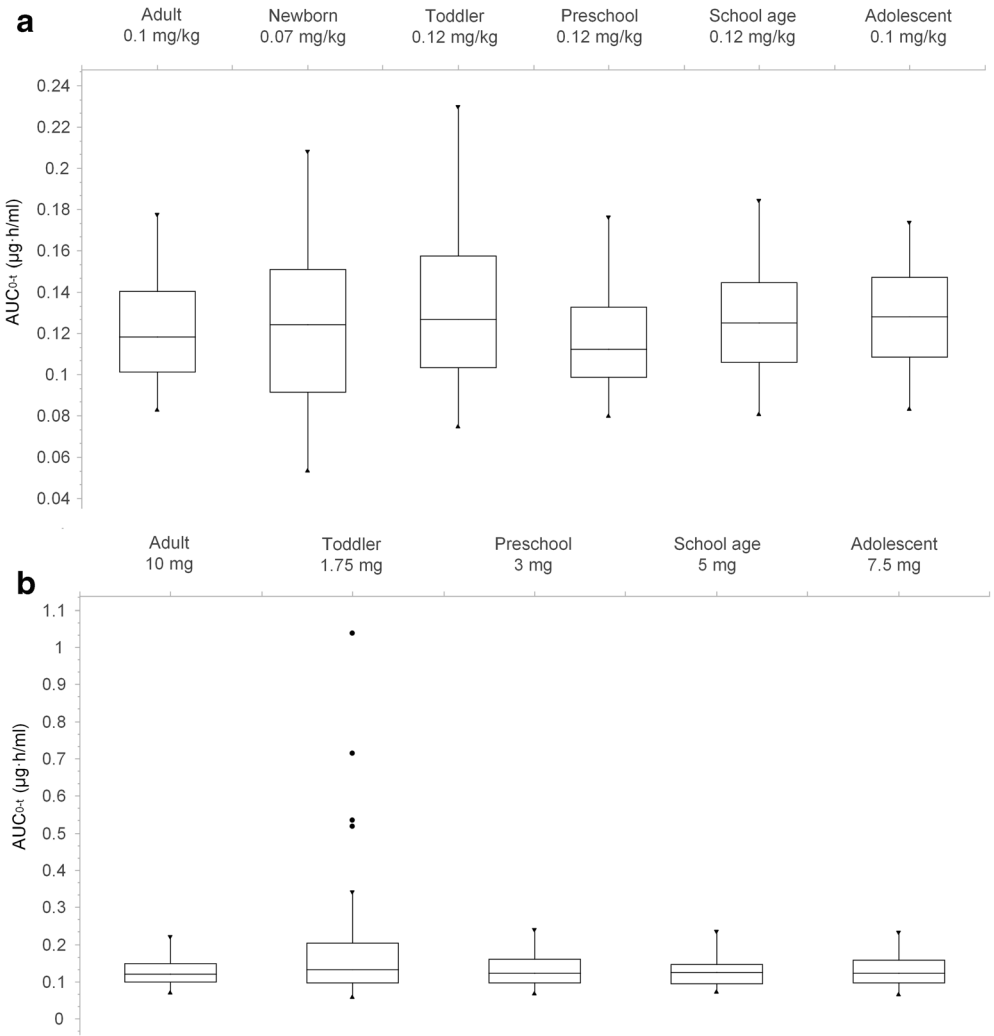

Fig. 5 The Box-Whisker analysis of predicted oxycodone exposure following intravenous and oral administration in the population of young adults and children at all age stages. The area under the time-concentration curve (AUC) from zero to 12 h was used as an indicator for intravenous dosing, while AUC from zero to 24 h and maximum concentration (Cmax) for oral dosing. The dots are outliers that are beyond the statistical range of variation.

have tried to develop the model through parameter refinement for i.v. and p.o. data simultaneously. Though two major metabolites, e.g. noroxycodone and oxymorphone, were also determined in many clinical PK studies, we did not choose to build PBPK model for the two compounds. As we mentioned in the introduction, the metabolites hardly cross the blood-brain barrier, thus their contribution to the effect of oxycodone is negligible. Besides, the lack of background information may lead to reduced reliability of the model. However, a previous study has developed a PBPK model for the two compounds (14). Compared to the previous study, the current PBPK model received a more comprehensive evaluation, as i.v. administration, CR formulation, and more clinical data were taken into account.

The current PBPK model for children calculated postnatal age with assumed full-term (postmenstrual age = 40 weeks) and different postmenstrual ages remain to be investigated. Postmenstrual age was a better descriptor of maturational changes than postnatal age (36). Though the PBPK model gave satisfactory fitting for the observed data in children over 6 months, the reliability of model-based prediction for the newborn and toddler should be further studied. On the other hand, previous studies reported a significant drug-drug interaction (DDI) when co-administered with CYP3A4 inhibitor ketoconazole and itraconazole, CYP2D6 strong inhibitor quinidine, and dual inhibitor telithromycin (21,37,38). Because of the maturation of physiology and metabolic enzymes, the potential DDI might be different in children compared with adults, perhaps in the extent of PK change. To give a prediction of DDI in children, the validated children models for oxycodone and those inhibitors must be developed, and the parameters for enzyme inhibition such as K_i and IC50 should be given. By far, the ketoconazole and itraconazole, and quinidine PBPK model had been validated for DDI prediction in adults, but these models have not been specified for children (39,40). Though lack of clinical DDI studies in children weakens the reliability of prediction, we think that such a DDI model will still provide valuable information to instruct oxycodone use in children when co-administered inhibitors are unavoidable.

In conclusion, we developed a whole-body pediatric PBPK model for oxycodone, a widely used opioid analgesic. The current model provides the opportunity for application of PBPK modeling to guide pediatric dose optimization of oxycodone in clinical practice and future PK studies.

ACKNOWLEDGMENTS AND DISCLOSURES

The authors thank current all members in Open Systems Pharmacology community in GitHub for providing proper instructions and advice during learning PBPK modeling. The authors report no conflicts of interest in this work.

REFERENCES

1. Hines RN. Developmental expression of drug metabolizing enzymes: impact on disposition in neonates and young children. Int J Pharm. 2013;452(1–2):3–7.
2. Bouwmeester NJ, Anderson BJ, Tibboel D, Holford NHG. Developmental pharmacokinetics of morphine and its metabolites in neonates, infants and young children. Brit J Anaesth. 2004;92(2):208–17.
3. Maharaj AR, Edginton AN. Physiologically based pharmacokinetic modeling and simulation in pediatric drug development. CPT Pharmacometrics Syst Pharmacol. 2014;3:e150.
4. Anderson BJ, Holford NHG. Mechanistic basis of using body size and maturation to predict clearance in humans. Drug Metab Pharmacok. 2009;24(1):25–36.
5. Luzon E, Blake K, Cole S, Nordmark A, Versantvoort C, Berglund EG. Physiologically based pharmacokinetic modeling in regulatory decision-making at the European medicines agency. Clin Pharmacol Ther. 2017;102(1):98–105.
6. Grimstein M, Yang Y, Zhang X, Grillo J, Huang SM, Zineh I, *et al.* Physiologically based pharmacokinetic modeling in regulatory science: an update from the U.S. Food and Drug Administration's Office of Clinical Pharmacology. J Pharm Sci. 2019;108(1):21–5.
7. Bianchi DW, Gillman MW. Addressing the impact of opioids on women and children. Am J Obstet Gynecol. 2019;221(2):123−+.
8. Biancofiore G. Oxycodone controlled release in cancer pain management. Ther Clin Risk Manag. 2006;2(3):229–34.
9. Kinnunen M, Piirainen P, Kokki H, Lammi P, Kokki M. Updated clinical pharmacokinetics and pharmacodynamics of oxycodone. Clin Pharmacokinet. 2019;58(6):705–25.
10. Lalovic B, Phillips B, Risler LL, Howald W, Shen DD. Quantitative contribution of CYP2D6 and CYP3A to oxycodone metabolism in human liver and intestinal microsomes. Drug Metab Dispos. 2004;32(4):447–54.
11. Romand S, Spaggiari D, Marsousi N, Samer C, Desmeules J, Daali Y, *et al.* Characterization of oxycodone in vitro metabolism by human cytochromes P450 and UDP-glucuronosyltransferases. J Pharm Biomed Anal. 2017;144:129–37.
12. Davis MP, Varga J, Dickerson D, Walsh D, LeGrand SB, Lagman R. Normal-release and controlled-release oxycodone: pharmacokinetics, pharmacodynamics, and controversy. Support Care Cancer. 2003;11(2):84–92.
13. Lalovic B, Kharasch E, Hoffer C, Risler L, Liu-Chen LY, Shen DD. Pharmacokinetics and pharmacodynamics of oral oxycodone in healthy human subjects: role of circulating active metabolites. Clin Pharmacol Ther. 2006;79(5):461–79.
14. Marsousi N, Daali Y, Rudaz S, Almond L, Humphries H, Desmeules J, *et al.* Prediction of metabolic interactions with oxycodone via CYP2D6 and CYP3A inhibition using a physiologically based pharmacokinetic model. CPT Pharmacometrics Syst Pharmacol. 2014;3:e152.
15. Willmann S, Lippert J, Sevestre M, Solodenko J, Fois F, Schmitt W. PK-Sim (R): a physiologically based pharmacokinetic'whole-body'model. Biosilico. 2003;4(1):121–4.
16. Rodgers T, Rowland M. Physiologically based pharmacokinetic modelling 2: predicting the tissue distribution of acids, very weak bases, neutrals and zwitterions. J Pharm Sci. 2006;95(6):1238–57.
17. Basit A, Radi Z, Vaidya VS, Karasu M, Prasad B. Kidney cortical transporter expression across species using quantitative proteomics. Drug Metab Dispos. 2019:dmd. 119.086579.
18. T'Jollyn H, Vermeulen A, Van Bocxlaer J. PBPK and its virtual populations: the impact of physiology on pediatric pharmacokinetic predictions of tramadol. AAPS J. 2018;21(1):8.
19. Nishimura M, Yaguti H, Yoshitsugu H, Naito S, Satoh T. Tissue distribution of mRNA expression of human cytochrome P450 isoforms assessed by high-sensitivity real-time reverse transcription PCR. Yakugaku Zasshi. 2003;123(5):369–75.
20. Nieminen TH, Hagelberg NM, Saari TI, Pertovaara A, Neuvonen M, Laine K, *et al.* Rifampin greatly reduces the plasma concentrations of intravenous and oral oxycodone. Anesthesiology. 2009;110(6):1371–8.
21. Saari TI, Gronlund J, Hagelberg NM, Neuvonen M, Laine K, Neuvonen PJ, *et al.* Effects of itraconazole on the pharmacokinetics and pharmacodynamics of intravenously and orally administered oxycodone. Eur J Clin Pharmacol. 2010;66(4):387–97.
22. Gronlund J, Saari TI, Hagelberg NM, Neuvonen PJ, Laine K, Olkkola KT. Effect of inhibition of cytochrome P450 enzymes 2D6 and 3A4 on the pharmacokinetics of intravenous oxycodone: a randomized, three-phase, crossover, placebo-controlled study. Clin Drug Investig. 2011;31(3):143–53.
23. Oshlack B, Chasin M, Minogue JJ, Kaiko RF. Controlled release oxycodone compositions. In: Google Patents; 1996.
24. Langenbucher F. Linearization of dissolution rate curves by the Weibull distribution. J Pharm Pharmacol. 1972;24(12):979–81.
25. Li Y, Sun D, Palmisano M, Zhou S. Slow drug delivery decreased total body clearance and altered bioavailability of immediate- and controlled-release oxycodone formulations. Pharmacol Res Perspect. 2016;4(1):e00210.
26. Biesdorf C, Martins FS, Sy SKB, Diniz A. Physiologically-based pharmacokinetics of ziprasidone in pregnant women. Br J Clin Pharmacol. 2019;85(5):914–23.
27. McNamara PJ, Alcorn J. Protein binding predictions in infants. AAPS PharmSci. 2002;4(1):E4.
28. Edginton AN, Schmitt W, Voith B, Willmann S. A mechanistic approach for the scaling of clearance in children. Clin Pharmacokinet. 2006;45(7):683–704.
29. Hayton WL. Maturation and growth of renal function: dosing renally cleared drugs in children. AAPS PharmSci. 2000;2(1):E3.
30. Kokki H, Rasanen I, Reinikainen M, Suhonen P, Vanamo K, Ojanpera I. Pharmacokinetics of oxycodone after intravenous, buccal, intramuscular and gastric administration in children. Clin Pharmacokinet. 2004;43(9):613–22.
31. El-Tahtawy A, Kokki H, Reidenberg BE. Population pharmacokinetics of oxycodone in children 6 months to 7 years old. J Clin Pharmacol. 2006;46(4):433–42.
32. Olkkola KT, Hamunen K, Seppala T, Maunuksela EL. Pharmacokinetics and ventilatory effects of intravenous oxycodone in postoperative children. Br J Clin Pharmacol. 1994;38(1):71–6.
33. Chen N, Aleksa K, Woodland C, Rieder M, Koren G. Ontogeny of drug elimination by the human kidney. Pediatr Nephrol. 2006;21(2):160–8.

34. Mooij MG, de Koning BA, Huijsman ML, de Wildt SN. Ontogeny of oral drug absorption processes in children. Expert Opin Drug Metab Toxicol. 2012;8(10):1293–303.
35. Kuepfer L, Niederalt C, Wendl T, Schlender JF, Willmann S, Lippert J, *et al.* Applied concepts in PBPK modeling: how to build a PBPK/PD model. CPT Pharmacometrics Syst Pharmacol. 2016;5(10):516–31.
36. Rhodin MM, Anderson BJ, Peters AM, Coulthard MG, Wilkins B, Cole M, *et al.* Human renal function maturation: a quantitative description using weight and postmenstrual age. Pediatr Nephrol. 2009;24(1):67–76.
37. Gronlund J, Saari T, Hagelberg N, Martikainen IK, Neuvonen PJ, Olkkola KT, *et al.* Effect of telithromycin on the pharmacokinetics and pharmacodynamics of oral oxycodone. J Clin Pharmacol. 2010;50(1):101–8.
38. Samer CF, Daali Y, Wagner M, Hopfgartner G, Eap CB, Rebsamen MC, *et al.* The effects of CYP2D6 and CYP3A activities on the pharmacokinetics of immediate release oxycodone. Br J Pharmacol. 2010;160(4):907–18.
39. Fenneteau F, Poulin P, Nekka F. Physiologically based predictions of the impact of inhibition of intestinal and hepatic metabolism on human pharmacokinetics of CYP3A substrates. J Pharm Sci. 2010;99(1):486–514.
40. Marsousi N, Desmeules JA, Rudaz S, Daali Y. Prediction of drug-drug interactions using physiologically-based pharmacokinetic models of CYP450 modulators included in Simcyp software. Biopharm Drug Dispos. 2018;39(1):3–17.
41. Moore C, Kelley-Baker T, Lacey J. Interpretation of oxycodone concentrations in oral fluid. J Opioid Manag. 2012;8(3):161–6.
42. Poyhia R, Olkkola KT, Seppala T, Kalso E. The pharmacokinetics of oxycodone after intravenous injection in adults. Br J Clin Pharmacol. 1991;32(4):516–8.
43. Gronlund J, Saari TI, Hagelberg NM, Neuvonen PJ, Olkkola KT, Laine K. Exposure to oral oxycodone is increased by concomitant inhibition of CYP2D6 and 3A4 pathways, but not by inhibition of CYP2D6 alone. Brit J Clin Pharmaco. 2010;70(1):78–87.
44. Gronlund J, Saari TI, Hagelberg N, Neuvonen PJ, Olkkola KT, Laine K. Miconazole oral gel increases exposure to oral oxycodone by inhibition of CYP2D6 and CYP3A4. Antimicrob Agents Chemother. 2011;55(3):1063–7.
45. Hagelberg NM, Nieminen TH, Saari TI, Neuvonen M, Neuvonen PJ, Laine K, *et al.* Voriconazole drastically increases exposure to oral oxycodone. Eur J Clin Pharmacol. 2009;65(3):263–71.
46. Liukas A, Kuusniemi K, Aantaa R, Virolainen P, Neuvonen M, Neuvonen PJ, *et al.* Plasma concentrations of oral oxycodone are greatly increased in the elderly. Clin Pharmacol Ther. 2008;84(4):462–7.
47. Nieminen TH, Hagelberg NM, Saari TI, Neuvonen M, Neuvonen PJ, Laine K, *et al.* Grapefruit juice enhances the exposure to oral oxycodone. Basic Clin Pharmacol Toxicol. 2010;107(4):782–8.
48. Nieminen TH, Hagelberg NM, Saari TI, Neuvonen M, Laine K, Neuvonen PJ, *et al.* St John's wort greatly reduces the concentrations of oral oxycodone. Eur J Pain. 2010;14(8):854–9.
49. Mandema JW, Kaiko RF, Oshlack B, Reder RF, Stanski DR. Characterization and validation of a pharmacokinetic model for controlled-release oxycodone. Br J Clin Pharmacol. 1996;42(6):747–56.
50. Webster LR, Bath B, Medve RA, Marmon T, Stoddard GJ. Randomized, double-blind, placebo-controlled study of the abuse potential of different formulations of oral oxycodone. Pain Med. 2012;13(6):790–801.
51. Setnik B, Bass A, Bramson C, Levy-Cooperman N, Malhotra B, Matschke K, *et al.* Abuse potential study of ALO-02 (extended-release oxycodone surrounding sequestered naltrexone) compared with immediate-release oxycodone administered orally to nondependent recreational opioid users. Pain Med. 2017;18(6):1077–88.
52. Benziger DP, Miotto J, Grandy RP, Thomas GB, Swanton RE, Fitzmartin RD. A pharmacokinetic/pharmacodynamic study of controlled-release oxycodone. J Pain Symptom Manag. 1997;13(2):75–82.
53. Reder RF, Oshlack B, Miotto JB, Benziger DD, Kaiko RF. Steady-state bioavailability of controlled-release oxycodone in normal subjects. Clin Ther. 1996;18(1):95–105.